Chemical Engineering Journal 413 (2021) 127528

Contents lists available at ScienceDirect

Chemical Engineering Journal

journal homepage: www.elsevier.com/locate/cej

How can accumulated organics and salts deteriorate the biological treatment unit in the printing and dyeing wastewater recycling system?

Xin Jin [a], Rui Wang [a], Pengkang Jin [a,*], Xuan Shi [a], Yong Wang [a], Lu Xu [a], Xiaochang Wang [a], Huining Xu [b]

[a] Key Lab of Northwest Water Resource, Environment and Ecology, MOE, Xi'an University of Architecture and Technology, Xi'an 710055, China
[b] Shaanxi Key Laboratory of Environmental Engineering, Xi'an University of Architecture and Technology, Xi'an 710055, China

ARTICLE INFO

Keywords:
Water and wastewater recycling
Pollutant accumulation
Microbial activity inhibition
Metabolism pathway

ABSTRACT

Wastewater recycling is an effective way to reduce the fresh water supply and pollutant discharge for industry. Nevertheless, wastewater recycling will inevitably lead to the accumulation of inorganic ions and organic pollutants, which can deteriorate the activated sludge system. A printing and dyeing wastewater (PDWW) recycling system was established in this study to investigate the mechanism of biological treatment system deterioration due to organic and inorganic pollutant accumulation. It was found that organic matter accumulation especially intermediate products of added dyes and auxiliaries is crucial for the biological treatment unit deterioration during the beginning of closed-loop PDWW recycling (first 40 days). In addition, inorganic salt accumulation, such as Ca^{2+}, Na^{+}, K^{+}, SO_4^{2-} and Cl^{-}, can make it even worse afterwards. The results indicated that phenylalanine metabolism, synthesis and degradation of ketone bodies, butanoate metabolism and pyruvate metabolism were the four most significantly influenced metabolic pathways in the PDWW recycling system attributed to the organic matter accumulation. In addition, accumulated inorganic salts could inhibit glycan biosynthesis and metabolism, xenobiotic biodegradation and metabolism and lipid metabolic pathways in the PDWW recycling system, which ultimately deteriorated the biological treatment system.

1. Introduction

Wastewater reclamation is one potential solution to meeting the growing global demand for dwindling freshwater supplies and pollution discharge [1]. With respect to water reclamation applications, reclaimed water is mostly considered for scenic environment uses, industrial uses and municipal miscellaneous uses. Among these end uses, industrial applications are one of the largest applications for reclaimed water, which represent over 30% of the total recycled water consumption [2,3]. On the one hand, the government has undertaken a series of measures and policies to encourage industries to conduct wastewater reclamation and recycling. On the other hand, internal water recycling within industrial parks and industrial enterprises has been greatly improved, e.g. the recycling rate should be higher than 30% and 20% in the Beijing-Tianjin-Hebei region and water-deficient area in China [4].

Different from reclaimed water used for municipal application, for industrial wastewater reuse, reclaimed water is always recycled e.g. cooling water, process water and boiler feed water [2]. Nevertheless, wastewater recycling will inevitably lead to the accumulation of inorganic ions and organic pollutants [5–7], which will result in the deterioration of upstream wastewater treatment and reclamation systems and in turn restrict the further increase in the recycling rate. It has been reported that the in the current practices of many wastewater recycling processes in China, the nonylphenol (NP) removal efficiency is typically not high enough which may result in the accumulation of NP in wastewater recycling system effluents [5]. It was also implied that gradual accumulation of retardant byproducts in repeatedly reused effluents through catalytic ozonation can lead to the adverse effects on the dyeing procedure, such as exhaustion and fixation stages [6].

It is well-known that increased inorganic salts can affect the removal performance for both anaerobic and aerobic biological processes [8–11]. Salinity may directly or indirectly inhibit cell division and enlargement and finally the growth, productivity and performance of wastewater treatment plants [12], and even at low inorganic salt levels, it can lead to water quality deterioration of the recycled water and thus lead to human health and ecological safety problems [13]. Nevertheless, organic

* Corresponding author at: No. 13, Yanta Road, Beilin District, Xi'an, China.
E-mail address: pkjin@hotmail.com (P. Jin).

https://doi.org/10.1016/j.cej.2020.127528
Received 11 August 2020; Received in revised form 21 October 2020; Accepted 23 October 2020
Available online 27 October 2020

pollutants can also accumulate in the effluent of the wastewater recycling system [5,7,14]. However, previous studies only investigated the effect of either certain artificially added organic matters or salts on the removal performance of biological treatment units in acyclic systems [8–11,13]. Unlike artificially added inorganic salts and organic matters in the acyclic system, little knowledge can be obtained about the characteristics of organic matter and salt accumulation in a water and wastewater recycling system.

There are considerable residual dissolved organic matters (DOM) in industrial wastewater effluent, such as non-biodegradable raw material, microbial products and other micropollutants [15–17]. Moreover, the addition of auxiliary chemicals during production in industry contains a certain amount of salts, which leads to a variety of inorganic ions [18,19]. Therefore, multiple organic compounds and inorganic salts will coexist in industrial wastewater effluent. However, the mechanism of the influence of pollutant accumulation in the recycling system on a biological treatment unit needs to be understood, and which kinds of pollutant accumulation (organic accumulation and salt accumulation) preferentially affect the wastewater recycling system still needs investigation. The critical types of organic matters or inorganic salts responsible for biological treatment system deterioration are unclear for the recycling system, and the top easily accumulated or most influential organic matters and inorganic salts need to be revealed.

As one of the most important pillar industries in China, the printing and dyeing industry exhibits high water consumption and pollution discharge [20,21]. To decrease the pollution discharge and fresh water consumption, policies were introduced by the Chinese government, which require that the recycling rate of PDWW should reach more than 40%. Therefore, in this study, printing and dyeing wastewater (PDWW) was applied as a typical industrial wastewater that contains a high content of dyes, textile auxiliaries and salts, which are potentially toxic and exhibit poor biodegradability [22,23]. In addition, a closed-loop PDWW recycling system was established aiming at 1) investigating the types of pollutants responsible for PDWW recycling system deterioration based on organic and inorganic pollutant accumulation characteristics analysis; 2) revealing the critical factors leading to the biological system inhibition according to constrained redundancy analysis; 3) elucidating the different inhibition mechanisms due to organic pollutant and inorganic salt accumulation in biological treatment unit.

2. Materials and methods

2.1. PDWW recycling system

A PDWW recycling system with a treatment capacity of 5 m^3/d was built, which includes a coagulation sedimentation tank, hydrolysis acidification tank, aerobic tank, secondary sedimentation tank and dissolved ozone flotation (DOF) process (Fig. 1). The detailed size and hydraulic retention time (HRT) of the PDWW system is shown in Table S1. The sludge from the anaerobic tank and aerobic tank was inoculated with the returned sludge from a wastewater treatment plant in the Tudian printing and dyeing industrial park in Zhejiang Province of China. The initial sludge concentration and DO of the aerobic tank were kept at 3000 mg/L and 2–3 mg/L, respectively. The sludge retention time (SRT) was set at 12 days.

The DOF process was put forward in our previous study [24]. The dimension of the DOF tank is Φ0.8 × 3.2 m with a processing capacity of 36 m^3/d in intermittent operation mode. Polyaluminium chloride (PAC) was added with dosage at a 60–100 mg/L. The ozone dissolving pressure was 0.4 MPa. The recycling ratio was 40%. In the DOF tank, ozone was used instead of air, which was generated by an ozone generator (CF-G-2–100 g, Guolin Co. Ltd., Qingdao, China). The maximum ozone productivity for a single generator was 100 g/h with an electric power of 2 kW. The generated ozone concentration was 25 mg/L_{air}. In order to avoid the influence of water temperature fluctuation on the microbial community structure and function, the raw water tank, hydrolysis acidification tank and aerobic tank in the experimental system were heated by hot water circulation and foam board insulation. The water temperature of the system was maintained at 30 ± 0.5 °C. In addition, the system is equipped with three 5-m^3 water distribution tanks. One water tank acts as an intermediate tank between the secondary sedimentation tank and the DOF reactor. The other two water tanks act as the raw water tank and treated water tank alternatively. Therefore, the total HRT of the system was 80 h (approximately 3.3 d) according to Table S1, and thus, it took 3.3 days to recycle the water once.

2.2. Simulated printing and dyeing wastewater

The synthetic printing and dyeing wastewater consists of mixed dyes, auxiliaries and nutrients, as shown in Table 1. The composition of synthetic PDWW is as follows with COD (Chemical oxygen demand): N: P = 200:5:1. The auxiliaries used were all from industrial products, which were close to the composition of the actual printing and dyeing wastewater. The main components of the levelling agent included aliphatic alcohol polyoxyethylene ether (AEO) and polystyrene phenol. The deoiling agent is a mixture of sodium polyacrylate, white mineral oil and AEO. The softener was a cationic compound of monoglyceride quaternary ammonium salt. To make the synthetic printing and dyeing wastewater more representative, three dyes, reactive red 3BE-M, disperse rutile S/5BL and disperse yellow brown 4RL, were added, which rank in the top three in the consumption by typical printing and dyeing enterprises. The molecular structure and chemical formula of these three dyes are shown in Table S2, and Table S3 shows the COD contribution of each component from simulated printing and dyeing wastewater. Among them, the COD contribution of the levelling agent was approximately 42%, which was the main source of COD. The total

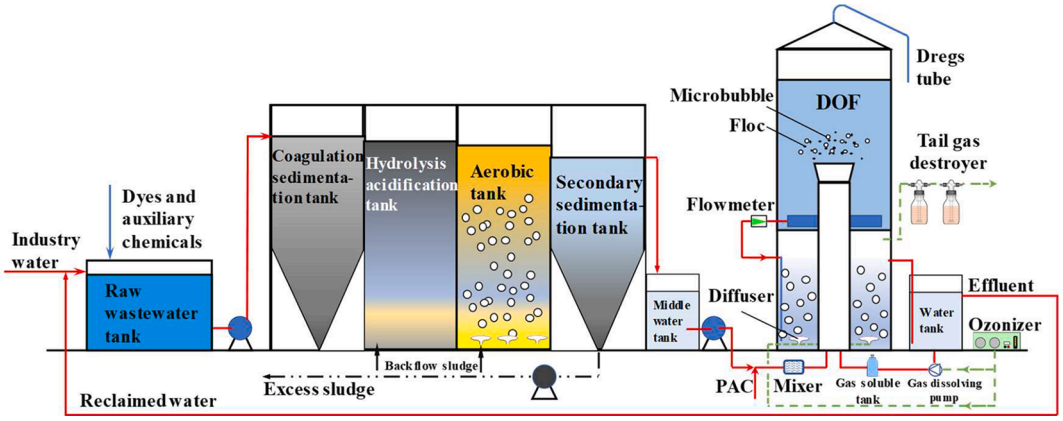

Fig. 1. Experimental setup of printing and dyeing wastewater recycling systems.

Table 1
Composition of the synthetic printing and dyeing wastewater.

Condition	Ingredients	Concentration (mg/L)	Condition	Ingredients	Concentration (mg/L)
Auxiliary	Levelling agent 2115	0.6‰(V/V)	Dyes	Reactive Red 3BE-M	9
	Degreasing agent AK-1016	0.2‰(V/V)		Disperse Yellow S/5BL	15
	Softener	0.7‰(V/V)		Disperse Brown 4RL	30
	CH_3COOH	0.2‰(V/V)	Trace elements solution	$FeSO_4$	2.4
	CH_3COONa	360		$MnCl_2$	0.32
	Na_2SO_4	80		NH_4Cl	14
	$CaCl_2$	14		$(NH_4)_2HPO_4$	8
	NaOH	80		$MgCl_2$	0.5

contribution of dyes was approximately 6.5%. Therefore, the COD in PDWW was mainly from AEO in the auxiliaries. In addition, the biological oxygen demand (BOD) of the raw synthetic printing and dyeing wastewater was 183 ± 21 mg/L.

2.3. Operation phases

The PDWW recycling system was operated in two phases, i.e., an air flotation treatment recycling phase (R_{DAF}) and a dissolved ozone flotation treatment recycling phase (R_{DOF}). Each phase included a 20-day startup. For every phase, there was a startup period. Auxiliary chemicals and dyes were added to domesticate microorganisms to adapt to dye degradation. The ozone dosage was 33 mg O_3/L in the R_{DOF} phase. During the recycling phase for R_{DAF} and R_{DOF}, the recycling ended when the MLSS was below 1000 mg/L or the specific oxygen uptake rate (SOUR) was below 1 g/(mg/L) [25]. The other operation conditions were consistent in the two phases, and the operation phases are shown in Table S4.

2.4. Analytical methods

Chemical oxygen demand (COD), MLSS, TDS and SVI were measured according to Chinese NEPA standard methods [26]. Conductivity was measured by a DDS-307 conductivity metre (INESA Scientific Instrument Co., Ltd., China). Proteins and polysaccharides were determined by the Folin method and anthrone colorimetric method, respectively [27].

Pollutant accumulating rates (K_a) were calculated using the following equation (Eq. (1)):

$$K_a = \frac{(c_t - c_0)}{t} \times 100\% \quad (1)$$

where K_a is the rate of pollutant accumulation (mg/L·d), c_0 is the pollutant concentration at the beginning of the recycling period (mg/L), c_t is the pollutant concentration at the end of the recirculating period (mg/L), and t is the recycling time (d).

Biomass activity was evaluated by determining the SOUR of activated sludge using Standard Method 1683 [28]. The SOUR determination of aerobic sludge was performed in a 500-mL biological oxygen demand (BOD) bottle. The BOD bottle was airproofed by a rubber stopper with an oxygen-sensing probe. The DO concentration was recorded by the oxygen-sensing probe at an interval of 30 s. The mixed liquor in the BOD bottle was mixed by a magnetic stirrer. The MLSS in the BOD bottle was regarded as constant during the whole experiment (30 min) due to the shorter operational time [11]. The SOUR was calculated from the DO-time curve based on the MLSS in the BOD bottle [29].

The organic species were analysed using GC–MS (Model 7890A-5975C, Agilent, USA) with an HP5-MS column (Text S1). AEO concentration was determined by HPLC using a Hypersil NH_2 column (Text S2). VFAs were analysed by GC (Text S3). In this study, the SMPs (proteins and polysaccharides) and VFAs (acetate, propionate, butyrate and valerate) were converted to COD according to stoichiometric conversion factors (1.5, 1.2, 1.07, 1.51, 1.82 and 2.04, respectively) [30]. The conversion of AEO to COD at 2.2 mg COD/mg AEO was obtained based on the experiments described in Text S4.

2.5. Microbial community and metagenome analysis

The sludge samples were sampled every 10 days. Each sample (V = 10 mL) was centrifuged at 3500 g for 10 min, after which the supernatant was discarded. The remaining sludge pellets were stored at −20 °C for a maximum of two months until DNA extraction. Genomic DNA of the sludge samples was extracted with the Power Soil DNA Kit (MO Biomedical, U.S.) and were sent to Novogene (Beijing, China) for shotgun 16S rDNA library construction using an Illumina Hiseq2500 platform [31].

By using bacterial primers 338F (50-ACT CCT ACG GGA GGC AGC AG-30) and 806R (50-GGA CTA CHV GGG TWT CTA AT-30), the V3-V4 region of the 16S rRNA gene was amplified, and each sample was marked by using the reverse primer including a 6-bp barcode [32].

Bacterial serial numbers were obtained from the ribosomal database project (http://rdp.cme.msu.edu/). Sequence comparisons were conducted with the BLAST search option in the NCBI nucleotide sequence database (http://www.ncbi.nlm.nih.gov/).

Protein sequences of the predicted genes were searched against the Nonsupervised Orthologous Groups (eggNOG, V3.0) [33], and the Kyoto Encyclopedia of Genes and Genomes (KEGG) function prediction was completed using I-Sanger based on 16S rRNA sequencing (http://www.isanger.com/).

Principle coordinate analysis (PCoA) plots were generated based on the weighted UniFrac distance matrices. Constrained redundancy analysis was performed using the Vegan package in R (2.13.1) to obtain the critical environmental parameters (i.e., AEO, VFAs, SMPs and micropollutants) that inhibited the microbial system. Specifically, distance-based redundancy analysis (db-RDA) via the capscale function in Vegan was performed to further analyse the obtained environmental factors in the unconstrained PCoA plot [32].

The metabolic dynamics of the activity sludge microbial communities were predicted by phylogenetic investigation of the communities by the reconstruction of unobserved states (PICRUSt) at the R_{DOF} phase according to the online protocol of the PICRUSt pipeline [34]. Analysis of variance (ANOVA) was conducted using SPSS 20.0 software to analyse the differences between various samples. The differences between samples with an adjusted $p < 0.05$ were considered statistically significant.

3. Results and discussion

3.1. Performance of the PDWW recycling system

The PDWW recycling systems for the R_{DAF} or R_{DOF} phase were continuously operated for 40 days and 100 days, respectively, and the variations of COD, conductivity and TDS are shown in Fig. 2. As shown in Fig. 2a, at the R_{DAF} recycling phase, the COD of raw wastewater and anaerobic tank effluent fluctuated and remained nearly constant at 750 mg/L and 450 mg/L, respectively, and no accumulation trend can was observed. Nevertheless, the COD of the secondary effluent increased

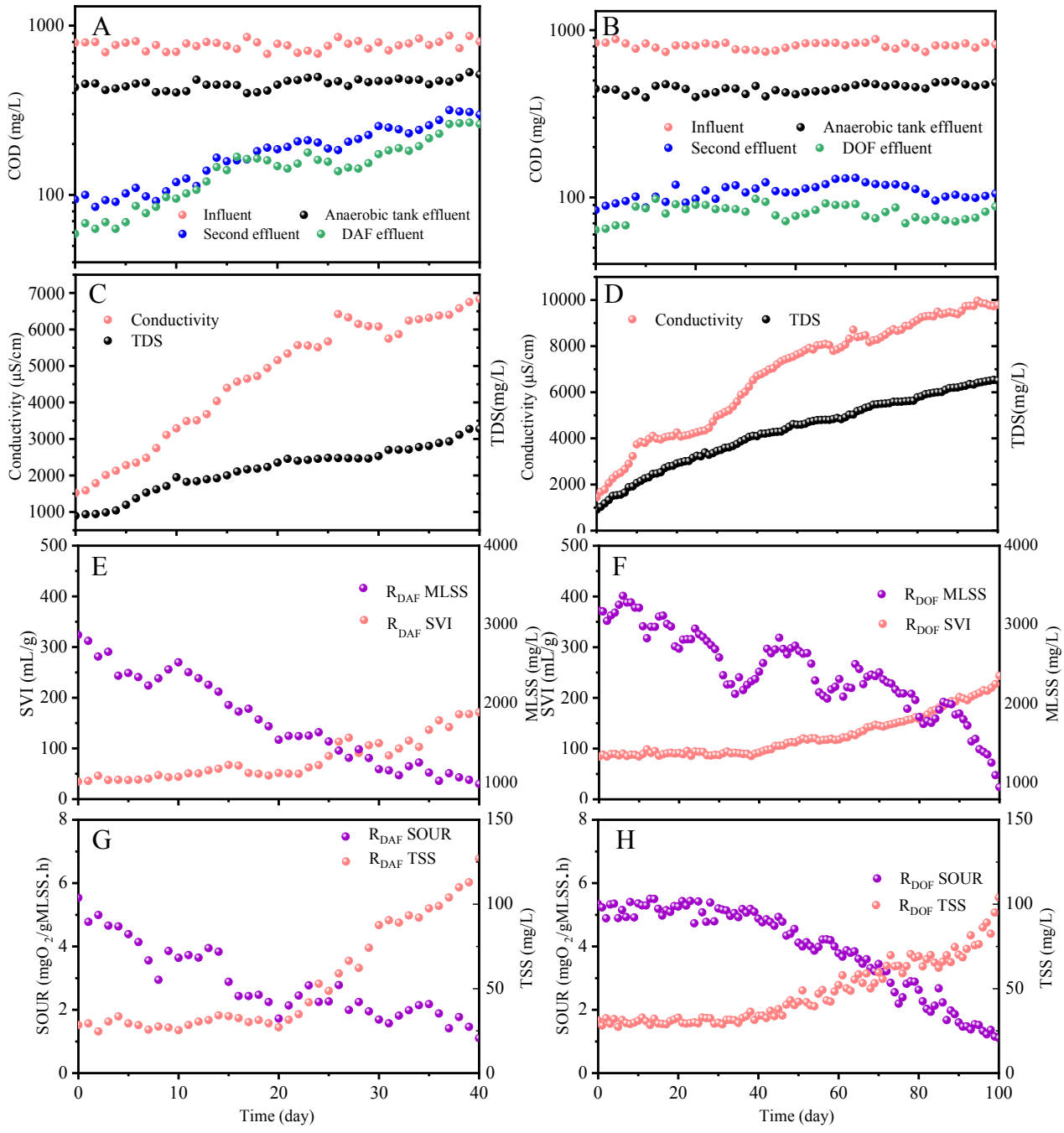

Fig. 2. Performance of the PDWW recycling system: effluent COD at the R_{DAF} (a) and R_{DOF} phases (b); effluent conductivity and TDS of DAF (c) and DOF (d); variation of MLSS and SVI in the aerobic activated sludge system at the R_{DAF} (e) and R_{DOF} phases (f); variation of SOUR and TSS in the aerobic activated sludge system at the R_{DAF} (g) and R_{DOF} phases (h).

from 93 mg/L to 309 mg/L (increased by 232%), and the COD accumulation rate was 5.4 mg/L·d. Fig. 2g shows that at the R_{DAF} phase, compared with the original activated sludge, the SOUR of the activated sludge in the 40th day decreased from 5.5 mgO_2/gMLSS h to 1.2 mgO_2/g MLSS h with a decrease rate of 78%. This also indicated that the accumulation of organic matter in the printing and dyeing wastewater recycling system inhibited the growth of microorganisms. However, at the R_{DOF} phase (Fig. 2b), the COD of the secondary effluent and DOF effluent fluctuated approximately 90 mg/L and 70 mg/L, respectively, and no significant accumulation was observed during the first 60 days. Therefore, DOF process can inhibit the accumulation of organic matter for the first 60 days compared with the DAF process.

In addition to the accumulation of organic matter during the PDWW recycling, the concentration of inorganic salts could also increase in the PDWW recycling system. Fig. 2c and show the variation of TDS and conductivity in the PDWW recycling system for the R_{DAF} and R_{DOF} phases, respectively. It can be seen that both the TDS and conductivity gradually increased during the PDWW recycling at almost the same accumulation rate. For both the R_{DAF} and R_{DOF} phases, the concentration of TDS increased from 960 mg/L to 3450 mg/L within 40 days, which increased approximately 2.6 times. In addition, the salinity also continued to increase from 40 to 100 days. Generally, a high salinity may affect the microbial community and function of the biological treatment unit [35,36]. Due to the same inorganic matter accumulation

performance for the R_{DAF} and R_{DOF} phases, the effect of inorganic matter accumulation on the PDWW recycling system is expected to be identical during first 40 days. Nevertheless, although the salinity increased within 40 days, the removal performance and biological treatment unit exhibited good conditions in the R_{DOF} phase according to Fig. 2. In addition, for the PDWW system, there are no specific treatment processes for salinity removal. Therefore, the salinity accumulation was not the critical factor for the deterioration of the PDWW recycling system in the first 40 days. Because the DOF process can effectively decrease the organic matter accumulation compared with the DAF process, the organic accumulation can be better controlled at the R_{DOF} phase. Therefore, the organic matter accumulation should be the critical factor for the PDWW recycling system operation within 40 days. Fig. 2e, f, g and h also confirm that the DOF process could maintain good operation of the activated sludge system within 60 days. In contrast, the DAF process could not maintain favourable condition for the activated sludge system, which was deteriorated in 40 days. In addition, according to Fig. 2b, although the DOF process can inhibit the organic matter accumulation for the first 60 days, the removal performance at the R_{DOF} phase started to deteriorate after 60 days, which indicated that inorganic matter accumulation began to have an adverse effect on the recycling system. If the inorganic salts do not accumulate in the system, the recycling system can always run in an equilibrium state due to the good organic accumulation inhibition performance of the DOF process.

3.2. Characteristics of accumulated pollutants in the PDWW recycling system

3.2.1. Characteristics of accumulated organics

Because of the biological treatment system deterioration due to organic matter accumulation within the first 40 days, the variation of organic matter composition in the PDWW secondary effluent was analysed in this study at the R_{DAF} and R_{DOF} phases, respectively (Fig. 3). Normally, the secondary effluent of the PDWW system is composed of SMPs and intermediate products derived from intermediate metabolites of dyes and auxiliaries. However, if the biological treatment system deteriorated, some originally added dyes and auxiliaries could appear in the PDWW effluent. Because the AEO was the highest contribution to the raw water COD according to Table S3, AEO was used as the typical organic representing originally added compositions.

According to Fig. 3a, the secondary effluent is mainly composed of SMPs and intermediate products, which are derived from intermediate metabolites of originally added dyes and auxiliaries during biological decomposition at the initial stage (0 days). However, for the R_{DAF} phase from the 20th to 40th days, the composition of the secondary effluent became four parts, i.e., SMPs, AEO, VFAs and intermediate products. Intermediate products were still the major component of the PDWW secondary effluent. In addition, the proportion of AEO increased from 1% to 6%, and the proportion of VFAs increased from 1% to 17%. Nevertheless, for the R_{DOF} phase, the composition of PDWW secondary effluent exhibited little variation. The AEO and VFAs were present in a very low proportion. The AEO is the major part of the levelling agent [37], and VFA is mainly generated from the anaerobic tank. AEO and VFA are very easy to degrade in the aerobic tank. The accumulation of AEO and VFAs indicated the deterioration of the aerobic activated sludge system at the R_{DAF} phase.

3.2.2. AEO, VFA and SMP analysis

Fig. 3b and c represent the accumulation performance of AEO and VFAs in the PDWW recycling system, respectively, at the R_{DAF} phase.

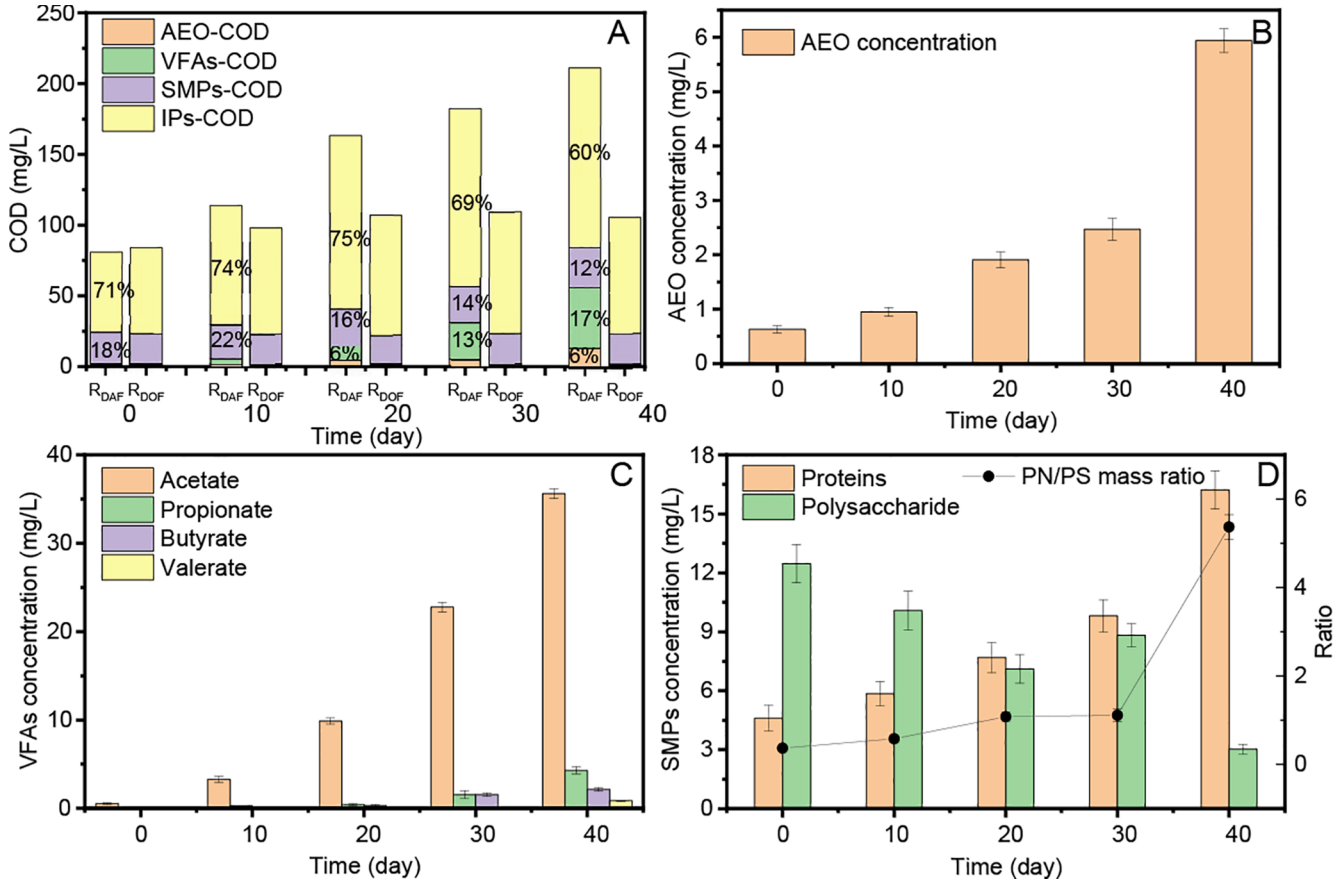

Fig. 3. Performance of DAF and DOF effluent in terms of equivalent SCOD concentrations of AEO, VFAs, SMPs and IPs (a). Variation of DAF effluent for AEO (b), VFAs (c) and PN, PS and PN/PS (d) at the R_{DAF} phase.

Fig. 3b and c show that for 0 days without PDWW recycling, AEO was lower than 1 mg/L, and the VFAs in the secondary effluent were lower than 0.6 mg/L. However, at the end of the cycles (40th day), the concentration of AEO in the secondary effluent increased to 5.94 mg/L (Fig. 3b). Although VFAs are easily degraded by microorganisms, they still accumulated in the PDWW system (Fig. 3c). Moreover, among the four kinds of VFAs, the accumulated VFAs were mainly composed of acetate, which was also added as an auxiliary in the synthetic PDWW, accounting for more than 85%. After 40 days of operation, the total concentration of VFAs increased to 42.9 mg/L.

SMPs, which primarily consist of proteins, polysaccharides and organic colloids, are derived from biological treatment and constitute a majority of the soluble DOM, which contributes to the high COD level in biotreated PDWW [38]. Further details regarding proteins and polysaccharides are presented in Fig. 3d. At the R_{DAF} phase, the protein in the secondary effluent increased from 4.6 mg/L to 16.1 mg/L within 40 days (Fig. 3d). Nevertheless, at the R_{DOF} phase, the protein of the secondary effluent was maintained approximately 7 mg/L. Under R_{DAF} conditions, the polysaccharides in the secondary effluent decreased from 12.5 mg/L to 3.1 mg/L, which can be due to the accumulation of pollutants and inhibition of microbial metabolic pathway activity [39]. However, at the R_{DOF} phase, the concentration of polysaccharides in the secondary effluent remained between 13.7 mg/L and 14.9 mg/L during the first 40 days. The PN/PS ratios in the second effluent at the R_{DAF} phase increased from 0.37 to 6.23, while they remained stable at the R_{DOF} phase. In general, when the environmental conditions are unfavourable, microorganisms produce a large quantity of exoenzymes, which leads to an increase in protein concentration in extracellular polymers (EPS) [11]. The PN/PS ratio in the secondary effluent at the R_{DAF} phase was greater than that at the R_{DOF} phase within 40 days. It can be suggested that PN at the R_{DAF} phase effluent was more sensitive to the accumulation of organic matters than PS.

3.2.3. Intermediate product analysis

To analyse the variation of intermediate metabolites of dyes and auxiliaries in the secondary effluent during the PDWW recycling, GC–MS analysis was introduced in this study. Fig. S1 shows the chromatograms of the effluent samples at 0th, 10th, 20th, 30th and 40th days at the R_{DAF} phase. The peaks represented different compounds, and only peaks with significant intensity were identified based on the NIST Library database with similarity above 80%. The detected compound names, chemical formulas and relativity peak areas are shown in Table S5. Most compounds can be grouped into alkanes, esters, benzene, alcohols, aldehydes and ketones, which are frequently found in biological treatment effluents and are related to the aerobic bacteria metabolism [38]. During the initial days, the total number of compounds in the secondary effluent was 76, and the number of these compounds in the secondary effluent is listed in Table S6.

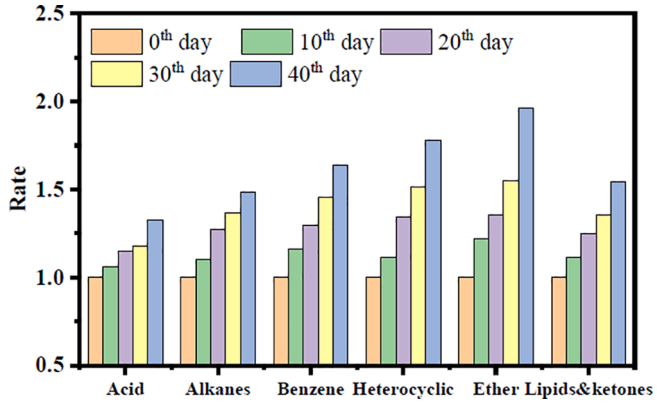

Fig. 4. Accumulation fold of detected organic intermediate metabolites in secondary effluent at different days.

Fig. 4 shows the equivalent accumulation fold of detected organic intermediate metabolites in the secondary effluent at different days based on Table S5. At the 40th day, ether, heterocyclic and benzene ring organic compounds exhibited high fold accumulation, which increased by 1.96, 1.78 and 1.64 times, respectively. As listed in Table S5, ethers include 2-butoxyethanol and ethylene glycol dodecyl ether. The former is a major component of dispersants, which can inhibit the activity of microorganisms [38].

In addition, among the heterocyclic compounds, quinoline exhibited the highest fold accumulation, which is one of the components of the dyeing auxiliaries [40]. The peak area of quinoline at the 40th day increased by 4.77 times compared with that at the beginning. Naphthalene, which is another type of heterocyclic compound, was the main organic compound with the highest peak area in the secondary effluent, which is a typical intermediate during the degradation and transformation of reactive dyes [41], and naphthalene accumulated 1.48 times within the 40 days.

In the PDWW recycling system, 2,4-di-*tert*-butylphenol had the highest concentration among the benzene compounds, which had adverse effects on flora and fauna [42] and caused environmental risk in water [34]. Additionally, the top three accumulation benzene compounds are phenylpyruvate (3.58 times), biphenyl (2.91 times) and 2-aminobenzene sulfonate (2.73 times). Moreover, aniline, which also belongs to benzene compounds, was strictly controlled according to the discharge standards of water pollutants for dyeing and finishing of the textile industry (GB 4287–2012) (<1 mg/L). At the R_{DAF} phase, aniline and dichloroaniline exhibited 1.43- and 1.91-fold accumulation, respectively (Table S5). It has been reported that 3,4-dichloroaniline (3,4-DCA), a type of raw material in the chemical industry, is widely used in the manufacturing of dyes [43], and it is known to accumulate at a hazardous level of approximately 0.68 μg/L in freshwater in the environment [44].

Various alkanes were detected in the secondary effluent of PDWW, such as C14, C16 and C28, which were also observed by analysing the degradation of AEO [37]. AEO was first hydrolysed to free fatty alcohol (FFA) and polyethylene glycol (PEG), and C12, C14 and C16 are considered as the by-products of FFA and PEG during biodegradation [37], which increased by 1.90, 1.21 and 1.53, respectively. The peak areas of other additives, such as surfactant (tridecane) and antistatic agent (9-octadecenamide), increased by 1.54 and 1.63 times, respectively.

3.2.4. Characteristics of accumulated inorganic ions

Because the addition of CH_3COONa, Na_2SO_4, $CaCl_2$ and NaOH as auxiliaries in the simulated PDWW, Na^+, Ca^{2+}, SO_4^{2-} and Cl^- exhibited higher concentrations compared with other ions according to Table 2. For the first 40 days, the same detected inorganic ions indicated almost the same accumulation rate at the R_{DAF} and R_{DOF} phases. However, based on Fig. 2 and the above discussion, the inorganic salt accumulation was not the crucial factor for the deterioration of the activated sludge system at the R_{DAF} phase. However, after 60 days, the removal performance of the PDWW system at the R_{DOF} phase started to be inhibited, which can be attributed to the inorganic ion accumulation. At the 100th day, the Na^+, Ca^{2+}, SO_4^{2-} and Cl^- concentrations reached 1989, 231.4, 806 and 2772 mg/L, respectively, according to Table 2. In addition, an inorganic matter accumulation model was built according to Fig. S2, and the detected inorganic matter accumulation is consistent with the established inorganic matter accumulation model (Text S5 and Fig. S3).

3.3. Critical accumulation factors for activated sludge systems

3.3.1. Organic pollutant accumulation

PCoA was applied to analyse the critical accumulation factor for the PDWW recycling system. From the PCoA plot (Fig. S4) representing the

Table 2
Concentration of inorganic ions for different operation days.

Item	Days	SO_4^{2-}	Cl^-	Na^+	K^+	Ca^{2+}	Mg^{2+}	Si	Sb	Fe	Mn
DAF	0	109	389	289	3.3	38.9	7.76	5.04	0.010	0.18	0.036
	10	264	590	674	4.4	67.4	6.32	3.54	0.032	0.27	0.049
	20	328	996	789	7.0	89.0	8.36	2.85	0.049	0.39	0.058
	30	306	1542	1030	7.5	103.0	7.00	2.12	0.050	0.48	0.058
	40	390	1709	1246	11.1	125.0	6.17	1.73	0.051	0.51	0.098
DOF	0	157	441	316	2.3	35.4	7.64	5.04	0.01	0.18	0.023
	20	286	1130	801	6.7	91.7	6.85	1.72	0.051	0.46	0.065
	40	424	1850	1300	12.4	129.5	5.42	1.75	0.052	0.52	0.088
	60	516	2121	1498	20.3	183.0	6.95	1.64	0.058	0.56	0.079
	80	768	2518	1816	17.9	204.6	9.65	1.68	0.055	0.98	0.093
	100	806	2772	1989	21.6	231.4	10.56	1.55	0.051	1.10	0.101

phylogenetic variation between microbial samples (i.e., based on the weighted UniFrac distance metric), it can be observed that the activated sludge samples at the R_{DAF} and R_{DOF} phases diverged considerably. The results of a constrained redundancy analysis (i.e., RDA) (Fig. 5a) showed that the intermediate metabolites of dyes and auxiliaries are the parameters that can best explain the deterioration of the activated sludge system observed in the PCoA diagram (Fig. S4). The first two axes of the RDA (i.e., RDA1 (87.2%) and RDA2 (8.94%)) explain approximately 94% of the phylogenetic variation shown by the first two axes of the unconstrained db-RDA plot (i.e., PC1 (77.84%) and PC2 (12.47%)) (Fig. 5b).

These constraining parameters were selected from measured environmental parameters because they were both significant (ANOVA test with $p < 0.05$) and non-redundant (VIF < 10) in the db-RDA. Therefore, the constrained redundancy analysis identified that 2,4-di-*tert*-butylphenol, 1-methyl-naphthalene and resorcinol exhibited the most significant influence on the variation in the microbial community structure observed during PDWW recycling at the R_{DAF} phase. In general, phenol is a kind of dyestuff intermediate that widely exists in printing and dyeing wastewater [45]. It was confirmed that 2,4-di-*tert*-butylphenol (DTBP) is an antioxidant compound that exhibits antibiofilm activity [46]. Protein, polysaccharides and eDNA components of EPS were inhibited significantly ($p < 0.05$) upon exposure to DTBP [47]. Resorcinol is the intermediate product of reactive dyes in the process of microbial degradation after desulfonation and denitrification [41]. Compared with the initial value, the relative peak area of resorcinol in the 40th day of the secondary effluent in the PDWW recycling system doubled (Table S5). Because of its high initial concentration and relatively large accumulation rate in PDWW, the activity inhibition of activated sludge by resorcinol was significant. Additionally, as one of the important PAHs, 1-methyl-naphthalene was also an intermediate product during the biological degradation of reactive dyes [41].

The accumulation of organic matters can lead to the variation of the microbial community at the R_{DAF} phase. Numbers of OTUs, Good's coverage, and the Shannon, Chao1, ACE and Simpson indices of aerobic and anaerobic sludge samples in the PDWW recycling system at the R_{DAF} phase (97% similarity) are shown in Table S7. Significant differences between the aerobic sludge at different days in terms of OTU ($p < 0.03$) and Chao1 ($p < 0.01$) can be observed in Table S7. In order to analyse the composition and abundance of the bacterial community structure, the composition and relative abundance changes for the bacterial community of aerobic and anaerobic sludge at the phylum and genus levels at the R_{DAF} phase can be seen in Fig. S5. A detailed description is provided in Text S6.

3.3.2. *Inorganic salt accumulation*

Among the eight detected ions, the K^+, Ca^{2+}, Na^+, SO_4^{2-} and Cl^- were the critical ions during the PDWW recycling for the deterioration of the aerobic activated sludge system at the R_{DOF} phase according to the redundance analysis (Fig. 6). Compared with other ions detected in the recycling system, these five types of ions exhibited higher contents and rates of accumulation, which inhibited the performance of the activated sludge system. Based on the analysis of the bacterial community (Fig. S6), the abundance of salt-tolerant microorganisms increased with increasing recycling days. It was reported that these salt-tolerant microorganisms will accumulate high concentrations of ions to balance the high osmotic pressure [48]. Therefore, the cellular plasm will be separated due to the high osmotic pressure [49,50], and the enzymatic

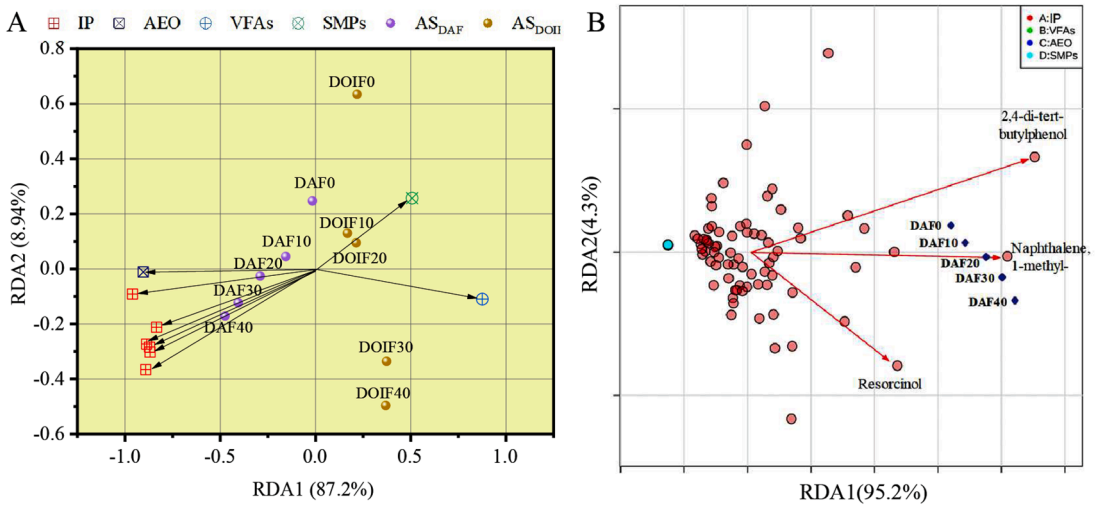

Fig. 5. Redundance analysis of inhibition of environmental parameters on microbial activity (RDA) (a); constrained distance-based redundancy analysis (db-RDA) (b) showing the environmental parameters that best explain the variation seen in the microbial community structure based on weighted UniFrac distances.

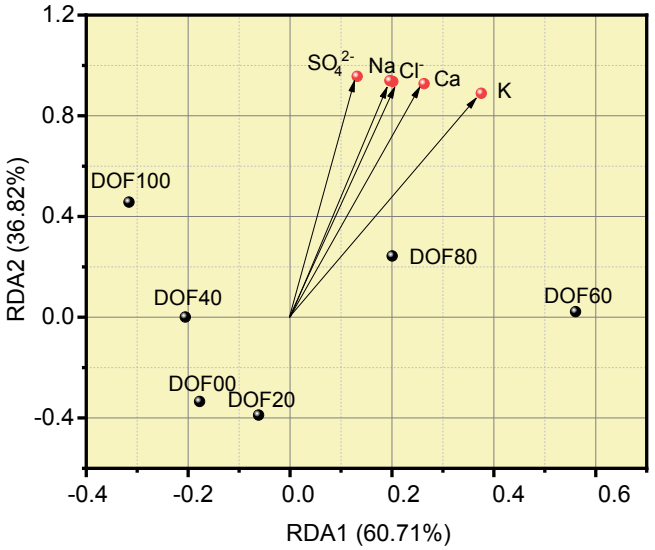

Fig. 6. Redundance analysis of accumulated inorganic ion inhibition on microbial activity (RDA) at the R_{DOF} phase.

activity can be severely inhibited in a highly salty environment [51].

At the R_{DOF} phase, the pollutant accumulation can also lead to the variations of microbial community. Numbers of OTUs, Good's coverage, and the Shannon, Chao1, ACE and Simpson indices of the aerobic and anaerobic sludge samples in the PDWW recycling system at the R_{DOF} phase (97% similarity) are shown in Table S8. Within the first 40 days, little difference between the aerobic sludge at different days in terms of OTU and Chao1 can be observed in Table S8, which indicates the stable operation for the first 40 days at the R_{DOF} phase. However, there were significant differences between aerobic sludge for the first 40 days and after 60 days, which indicated the deteriorated operation performance for the aerobic activated sludge system. In order to analyse the composition and abundance of the bacterial community structure, the detailed composition and relative abundance changes for the bacterial community of the aerobic and anaerobic sludge at the phylum and genus level at the R_{DOF} phase can be seen in Fig. S6. A detailed description is provided in Text S6.

3.4. Biological activity inhibitory mechanism

3.4.1. Microbial community function inhibition

For functional annotation, reads were assembled into contigs, and genes were subsequently predicted from the contigs and functionally annotated through the KEGG databases. The predicted genes fell into four major functional groups of the genes: "metabolism", "genetic information processing", "environmental information processing" and "cellular processes" with corresponding numbers of genes of 86030 ± 8200, 23673 ± 3094, 22208 ± 1539, and 17847 ± 1303, respectively, at the beginning of the R_{DAF} phase according to Fig. S7a. In the "metabolism" group, the genes matched to the amino acid metabolism exhibited the highest (25622 ± 2364), followed by carbohydrate metabolism (23736 ± 2214) and energy metabolism (19484 ± 1807). Within 40 days at the R_{DAF} phase, the highest gene number downregulation in the amino acid metabolism was Lysine biosynthesis with downregulation of 14.66%. Pentose and glucuronate interconversions exhibited the highest downregulation (16.88% downregulation) among the carbohydrate metabolism, and the gene number of oxidative phosphorylation decreased the most significantly in the energy metabolism (13.53% downregulation).

The numbers of matched genes of the four functional groups were 349964 ± 25000, 96815 ± 6541, 91167 ± 5557, and 7237 ± 4896, accounting for 57.3–61.1%, 10.9–11.9%, 10.7–11.5%, and 8.3–9.4%, respectively at the beginning of the R_{DOF} phase. According to Fig. S7b, the highest abundant genes in the metabolism category were "carbohydrate metabolism" (10383 ± 7891, 9.6–11.4%), followed by "amino acid metabolism" (97091 ± 7051, 9.9–11.3%) and "energy metabolism" (80237 ± 5500, 9.5–10.2%). As shown in Fig. S7b, the KEGG pathway analysis indicated that most of the functional genes increased in the first 40 days, and then decreased from the the 40th to 100th days. It can be speculated that at the initial stage of the recycling at the R_{DOF} phase, microorganisms gradually adapted to the gradually increasing salinity environment, and the activated sludge system started to deteriorate due to functional inhibition afterwards. Within 100 days at the R_{DOF} phase, the number of matched genes in the galactose metabolism exhibited the highest downregulation (17.8%) in carbohydrate metabolism. In amino acid metabolism, the number of matched genes related to phenylalanine metabolism decreased the most (13.9%). The number of oxidative phosphorylation functional genes decreased by 15.6%, which was the highest downregulation in energy metabolism.

3.4.2. Metabolic pathway analysis

To further reveal the effect of accumulated organic matters on bacterial metabolic activities, a metabolic profiling technique was adopted. Because the intermediate metabolic products of dyes and auxiliaries are critical factor for the deterioration of activated sludge system at the R_{DAF} phase, 76 kinds of detected intermediate metabolic products were further analysed. After the one-way ANOVA assessment, among the 76 GC–MS detected intermediate metabolic products, 66 metabolites exhibited significance during the PDWW recycling (Fig. 7a). According to the volcano plot ($p < 0.05$, fold change greater than 1.5) (Fig. 7b), the number of significantly changed metabolites was reduced to 39. The PCA diagram (Fig. 7c) also indicated that there are significant changes in microbial metabolism at the early and late days. Meanwhile, based on MetaboAnalyst online programming, the metabolic pathway activities could be calculated (Fig. 7d) [52,53]. Fig. 7d shows that two pathways were influenced significantly due to the discrimination of the two sets of samples (pathway impact > 0.6, and -log (p-value) > 5), which were phenylalanine metabolism and synthesis and degradation of ketone bodies. These two pathways are closely related to the amino acid metabolism and lipid metabolism, respectively [53,54]. In addition, it should be noted that the other two influenced pathways are butanoate metabolism and pyruvate metabolism, both of which are closely related to carbon metabolism. Therefore, the details of the four influenced metabolic pathways were analysed according to the KEGG database. The details of phenylalanine, synthesis and degradation of ketone bodies, butanoate metabolism and pyruvate metabolism pathway are shown in Fig. 8 for 0 and 40 days.

The pathways of phenylalanine metabolism were associated with amino acid metabolism [55]. Fig. 8a shows that the gene numbers corresponding to phenyl acetaldehyde dehydrogenase (feab) and aromatic amino acid decarboxylase (AADC) were obviously downregulated in the phenylalanine pathway. feaB is a kind of oxidoreductase that can metabolize aromatic compounds. Additionally, AADC catalyses decarboxylation reactions such as phenylalanine to phenethylamine in Fig. 8a. It has been reported that phenylalanine cannot be synthesized independently, which is an important compound involved in carbohydrate and lipid metabolism [54]. The decrease in phenylalanine metabolic pathway activity will have a direct impact on microbial productivity. In this study, phenylpyruvate related to phenylalanine metabolism accumulated (increased 2.6 fold). In accordance with this, the activity of synthesis and degradation of ketone bodies shown in Fig. 8b was also significantly impacted, which belongs to lipid metabolism. Fig. 8b clearly shows that hydroxymethylglutaryl-CoA synthase (EC 2.3.3.10) had the largest downregulated in the synthesis and degradation of ketone bodies. EC 2.3.3.10 is an enzyme that catalyses the reaction in which acetyl-CoA condenses with acetoacetyl-CoA to form 3-hydroxy-3-methylglutaryl-CoA (HMG-CoA).

Fig. 8c and d show the butyrate metabolism and pyruvate

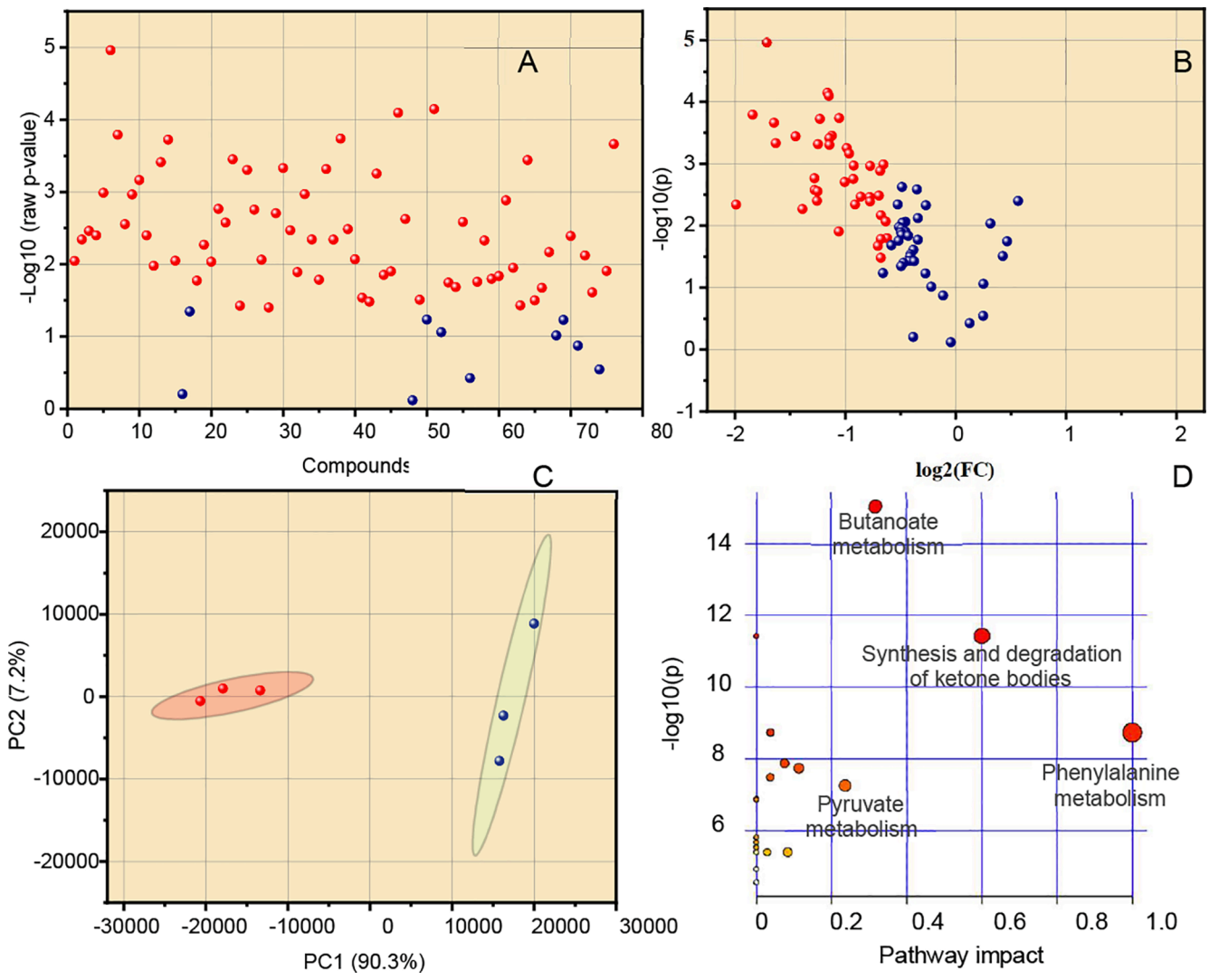

Fig. 7. Statistical analysis of metabolites extracted from the second effluent during 0th and the 40th days: (a) One-way ANOVA analysis, red dots represent metabolites with significant difference between the two groups. (b) Volcano plot, red dots represent metabolites of the 0th day sample upregulated more than 1.5 times and $p < 0.05$ compared with those of the 40th day, whereas blue dots represent metabolites of the 0th-day sample that was downregulated more than 1.5 times and $p < 0.05$ compared with those of the 40th day. (c) PCA analysis. (d) The impact and significance of metabolic pathways for the discrimination between the 0th and 40th day sample R-low metabolomics profiles as analysed by MetaboAnalyst. (For interpretation of the references to colour in this figure legend, the reader is referred to the web version of this article.)

metabolism pathways, respectively, both of which belong to carbohydrate metabolism. Fig. 8c shows that ACSM and PTB are the two enzymes with the largest downregulated genes, which correspond to the synthesis of medium chain acyl CoA and the transfer of phosphobutyryl, respectively. ACSM belongs to the family of ligases, specifically those forming carbon-sulfur bonds as acid-thiol ligases. PTB belongs to the family of transferases, specifically those acyltransferases transferring groups other than aminoacyl groups. Fig. 8d shows the change in the synthesis and degradation of acetic acid in the pyruvate metabolism pathway. There are 7 pathways involved in the acetic acid pathway, and the number of genes corresponding to 6 pathways is downregulated, which results in the inhibition of carbohydrate degradation activity and significant accumulation of organic matter in the secondary effluent.

The general metabolic pathway variation at 0, 20, 40, 60, 80 and 100 days at the R_{DOF} phase is shown in Fig. 9. In addition to the first day, the influenced metabolic pathways are denoted with different colours. According to Fig. 9, the most influenced metabolic pathways were related to glycan biosynthesis and metabolism at the 20th day. Furthermore, the number of influenced metabolic pathways increased obviously from the 20th to 60th days, which are mainly regarded as glycan biosynthesis and metabolism as well as xenobiotics biodegradation and metabolism. From the 80th day, lipid metabolic pathways began to be inhibited. The key genes coding for the metabolic pathways are shown in Table S9 ($p < 0.05$).

4. Conclusion

The pollutant accumulation characteristics during PDWW closed-loop recycling were investigated based on the established PDWW recycling system. It was found that the activated sludge system in the PDWW recycling system will be first affected by organic matter accumulation rather than inorganic ions. The accumulated organic pollutants can be classified as fatty alcohol polyoxyethylene ether (AEO), volatile fatty acids (VFA), soluble microbial products (SMPs) and other organic matter that is mainly composed of organic dye intermediates. According to GC/MS and constrained distance-based redundancy analysis (db-RDA), organic dye intermediates are the critical types of organic matter responsible for activated sludge system deterioration. Based on MetaboAnalyst online programming, phenylalanine metabolism, synthesis and degradation of ketone bodies, butanoate metabolism and pyruvate

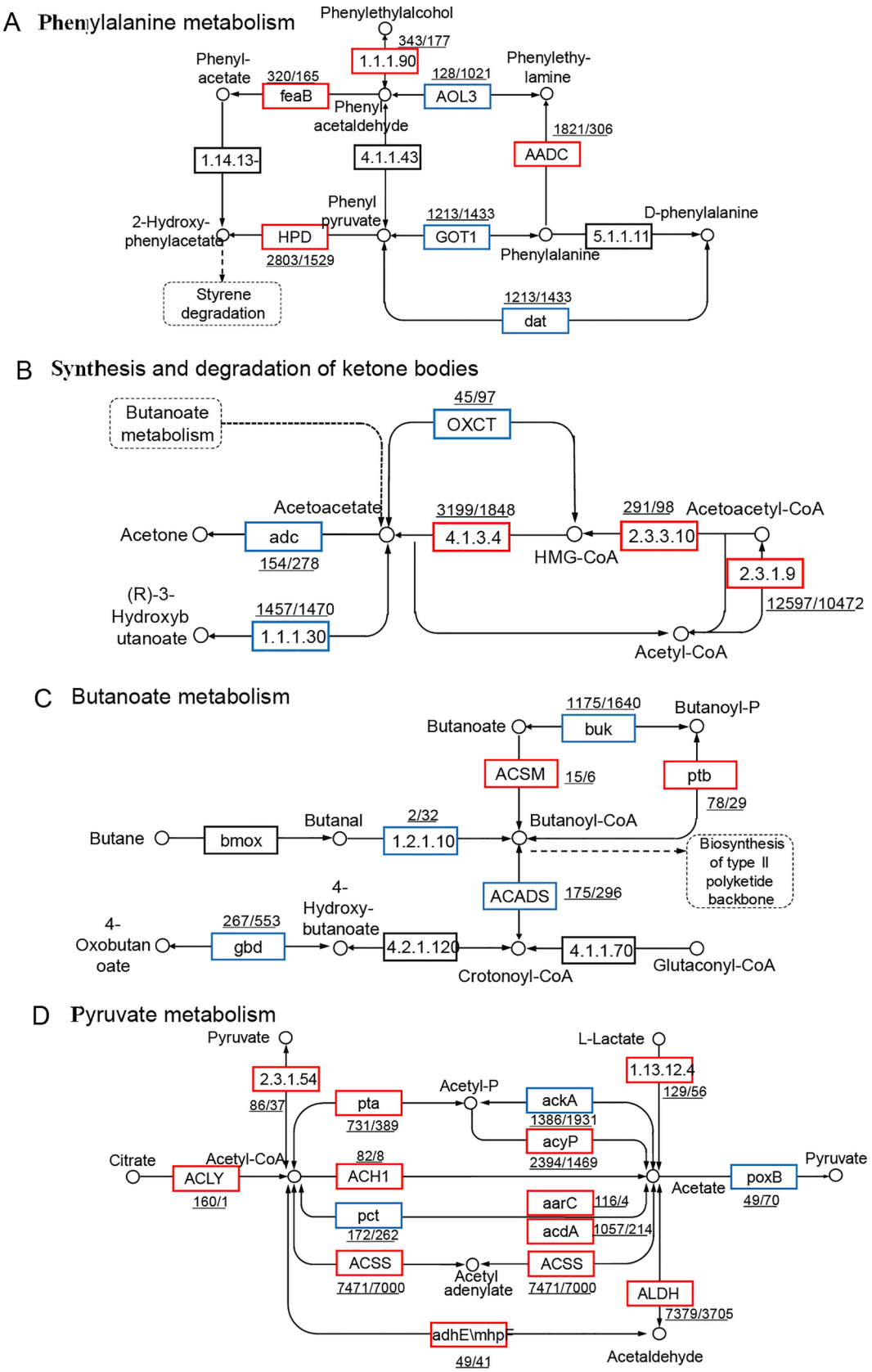

Fig. 8. Metabolomic fold variation for the 40th-day activated sludge sample compared with the 0th-day samples for relevant pathways at the R_{DAF} phase. The metabolites upregulated and downregulated are marked in blue and red, respectively. The metabolites that could not be recognized are marked in black. (For interpretation of the references to colour in this figure legend, the reader is referred to the web version of this article.)

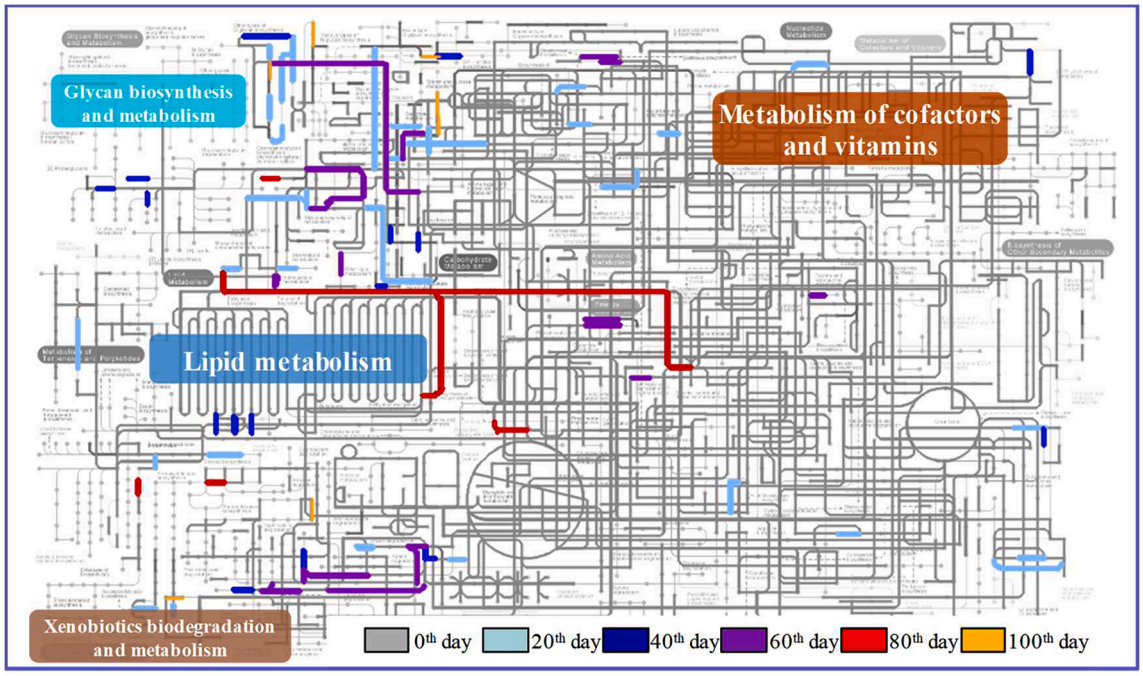

Fig. 9. Metabolic pathways in the aerobic activated sludge system at the R_{DOF} phase.

metabolism were determined to be the four most significantly influenced metabolic pathways in the PDWW recycling system. In addition, although the organic accumulation can be mitigated at the R_{DOF} phase within 40 days, inorganic ions began to inhibit the removal performance of the recycling system after 60 days. It was revealed that the lipid metabolic pathways as well as xenobiotic biodegradation and metabolism and glycan biosynthesis and metabolic pathways were influenced due to the accumulated inorganic salts at the R_{DOF} phase, which ultimately deteriorated the biological treatment system.

Declaration of Competing Interest

The authors declare that they have no known competing financial interests or personal relationships that could have appeared to influence the work reported in this paper.

Acknowledgements

This work was supported by the National Key R&D Program of China (No. 2019YFB2103003), the National Natural Science Foundation of China (No. 51708443), the Key Research and Development Project of Shaanxi Province (2019ZDLSF05-03) and the New Style Think Tank of Shaanxi Universities.

Appendix A. Supplementary data

Supplementary data to this article can be found online at https://doi.org/10.1016/j.cej.2020.127528.

References

[1] D.M. Glick, J.L. Goldfarb, W. Heiger-Bernays, D.L. Kriner, Public knowledge, contaminant concerns, and support for recycled Water in the United States, Resour. Conserv. Recycl. 150 (2019), 104419.
[2] Z. Chen, Q. Wu, G. Wu, H.-Y. Hu, Centralized water reuse system with multiple applications in urban areas: Lessons from China's experience, Resour. Conserv. Recycl. 117 (2017) 125–136.
[3] L. Yi, W. Jiao, X. Chen, W. Chen, An overview of reclaimed water reuse in China, J. Environ. Sci. 23 (2011) 1585–1593.
[4] MEE, Standard for National Demonstration Eco-industrial Parks, in, Standards Press of China (2016).
[5] R.-X. Hao, Y.-W. Zhou, S.-Y. Cheng, J.-B. Li, M. Zhao, X. Chen, N. Yao, The accumulation of nonylphenol in a wastewater recycling process, Chemosphere 70 (2008) 783–790.
[6] E. Hu, S. Shang, X.-M. Tao, S. Jiang, K.-L. Chiu, Regeneration and reuse of highly polluting textile dyeing effluents through catalytic ozonation with carbon aerogel catalysts, J. Cleaner Prod. 137 (2016) 1055–1065.
[7] G. Yamin, M. Borisover, E. Cohen, J. van Rijn, Accumulation of humic-like and proteinaceous dissolved organic matter in zero-discharge aquaculture systems as revealed by fluorescence EEM spectroscopy, Water Res. 108 (2017) 412–421.
[8] L. Chen, Q. Hu, X. Zhang, Z. Chen, Y. Wang, S. Liu, Effects of salinity on the biological performance of anaerobic membrane bioreactor, J. Environ. Manage. 238 (2019) 263–273.
[9] J.D. Muñoz Sierra, M.J. Oosterkamp, W. Wang, H. Spanjers, J.B. van Lier, Impact of long-term salinity exposure in anaerobic membrane bioreactors treating phenolic wastewater: Performance robustness and endured microbial community, Water Res. 141 (2018) 172–184.
[10] Y. Wang, J. Chen, S. Zhou, X. Wang, Y. Chen, X. Lin, Y. Yan, X. Ma, M. Wu, H. Han, 16S rRNA gene high-throughput sequencing reveals shift in nitrogen conversion related microorganisms in a CANON system in response to salt stress, Chem. Eng. J. 317 (2017) 512–521.
[11] Z. Wang, M. Gao, Z. She, S. Wang, C. Jin, Y. Zhao, S. Yang, L. Guo, Effects of salinity on performance, extracellular polymeric substances and microbial community of an aerobic granular sequencing batch reactor, Sep. Purif. Technol. 144 (2015) 223–231.
[12] K. Bencherif, A. Boutekrabt, J. Fontaine, F. Laruelle, Y. Dalpè, A. Lounès-Hadj Sahraoui, Impact of soil salinity on arbuscular mycorrhizal fungi biodiversity and microflora biomass associated with Tamarix articulata Vahll rhizosphere in arid and semi-arid Algerian areas, Sci. Total Environ. 533 (2015) 488–494.
[13] Y. Tian, J. Zhang, D. Wu, Z. Li, Y. Cui, Distribution variation of a metabolic uncoupler, 2,6-dichlorophenol (2,6-DCP) in long-term sludge culture and their effects on sludge reduction and biological inhibition, Water Res. 47 (2013) 279–288.
[14] L. Jidong, H. Yanling, Z. Jinwei, D. Wenjing, Accumulation of dissolved and colloidal substances in water recycled during papermaking, Chem. Eng. J. 168 (2011) 604–609.
[15] B.K. Shanmugam, S.N. Easwaran, A.S. Mohanakrishnan, C. Kalyanaraman, S. Mahadevan, Biodegradation of tannery dye effluent using Fenton's reagent and bacterial consortium: A biocalorimetric investigation, J. Environ. Manage. 242 (2019) 106–113.
[16] N. Zhu, L. Gu, H. Yuan, Z. Lou, L. Wang, X. Zhang, Degradation pathway of the naphthalene azo dye intermediate 1-diazo-2- naphthol-4-sulfonic acid using Fenton's reagent, Water Res. 46 (2012) 3859–3867.
[17] X.-A. Ning, M.-Q. Lin, L.-Z. Shen, J.-H. Zhang, J.-Y. Wang, Y.-J. Wang, Z.-Y. Yang, J.-Y. Liu, Levels, composition profiles and risk assessment of polycyclic aromatic hydrocarbons (PAHs) in sludge from ten textile dyeing plants, Environ. Res. 132 (2014) 112–118.
[18] J. Dasgupta, J. Sikder, S. Chakraborty, S. Curcio, E. Drioli, Remediation of textile effluents by membrane based treatment techniques: A state of the art review, J. Environ. Manage. 147 (2015) 55–72.
[19] L. Bilińska, K. Blus, M. Gmurek, S. Ledakowicz, Coupling of electrocoagulation and ozone treatment for textile wastewater reuse, Chem. Eng. J. 358 (2019) 992–1001.

[20] L. Zhou, K. Xu, X. Cheng, Y. Xu, Q. Jia, Study on optimizing production scheduling for water-saving in textile dyeing industry, J. Cleaner Prod. 141 (2017) 721–727.
[21] K. Vikrant, B.S. Giri, N. Raza, K. Roy, K.-H. Kim, B.N. Rai, R.S. Singh, Recent advancements in bioremediation of dye: Current status and challenges, Bioresour. Technol. 253 (2018) 355–367.
[22] C.R. Holkar, A.J. Jadhav, D.V. Pinjari, N.M. Mahamuni, A.B. Pandit, A critical review on textile wastewater treatments: Possible approaches, J. Environ. Manage. 182 (2016) 351–366.
[23] H. Chen, Y. Liu, X. Xu, M. Sun, M. Jiang, G. Xue, X. Li, Z. Liu, How does iron facilitate the aerated biofilter for tertiary simultaneous nutrient and refractory organics removal from real dyeing wastewater? Water Res. 148 (2019) 344–358.
[24] X. Jin, P. Jin, X. Wang, A study on the effects of ozone dosage on dissolved-ozone flotation (DOF) process performance, Water Sci. Technol. 71 (2015) 1423–1428.
[25] K. Kawasaki, S. Maruoka, R. Katagami, C.P. Bhatta, D. Omori, A. Matsuda, Effect of initial MLSS on operation of submerged membrane activated sludge process, Desalination 281 (2011) 334–339.
[26] NEPA, Water and Wastewater Monitoring Methods, in, Chinese Environmental, Science Publishing House, Beijing, China, 2002.
[27] G.U. Semblante, F.I. Hai, H. Bustamante, N. Guevara, W.E. Price, L.D. Nghiem, Effects of iron salt addition on biosolids reduction by oxic-settling-anoxic (OSA) process, Int. Biodeterior. Biodegrad. 104 (2015) 391–400.
[28] APHA, Standard Methods for the Examination of Water and Wastewater, in, American Public Health Association/American Water Works Association/Water Environment Federation, Washington DC, 2005.
[29] W. Luo, H.V. Phan, M. Xie, F.I. Hai, W.E. Price, M. Elimelech, L.D. Nghiem, Osmotic versus conventional membrane bioreactors integrated with reverse osmosis for water reuse: Biological stability, membrane fouling, and contaminant removal, Water Res. 109 (2017) 122–134.
[30] S.F. Aquino, D.C. Stuckey, Soluble microbial products formation in anaerobic chemostats in the presence of toxic compounds, Water Res. 38 (2004) 255–266.
[31] N.J. Loman, R.V. Misra, T.J. Dallman, C. Constantinidou, S.E. Gharbia, J. Wain, M. J. Pallen, Performance comparison of benchtop high-throughput sequencing platforms, Nat. Biotechnol. 30 (2012) 434–439.
[32] Z.-R. Chu, K. Wang, X.-K. Li, M.-T. Zhu, L. Yang, J. Zhang, Microbial characterization of aggregates within a one-stage nitritation–anammox system using high-throughput amplicon sequencing, Chem. Eng. J. 262 (2015) 41–48.
[33] S. Powell, K. Forslund, D. Szklarczyk, K. Trachana, A. Roth, J. Huerta-Cepas, T. Gabaldón, T. Rattei, C. Creevey, M. Kuhn, L.J. Jensen, C. von Mering, P. Bork, eggNOG v4.0: nested orthology inference across 3686 organisms, Nucleic Acids Res. 42 (2013) D231–D239.
[34] B. Li, X. Hu, R. Liu, P. Zeng, Y. Song, Occurrence and distribution of phthalic acid esters and phenols in Hun River Watersheds, Environ. Earth Sci. 73 (2015) 5095–5106.
[35] X. Song, J. McDonald, W.E. Price, S.J. Khan, F.I. Hai, H.H. Ngo, W. Guo, L. D. Nghiem, Effects of salinity build-up on the performance of an anaerobic membrane bioreactor regarding basic water quality parameters and removal of trace organic contaminants, Bioresour. Technol. 216 (2016) 399–405.
[36] R. Campo, S.F. Corsino, M. Torregrossa, G. Di Bella, The role of extracellular polymeric substances on aerobic granulation with stepwise increase of salinity, Sep. Purif. Technol. 195 (2018) 12–20.
[37] A. Szymanski, B. Wyrwas, Z. Swit, T. Jaroszynski, Z. Lukaszewski, Biodegradation of fatty alcohol ethoxylates in the continuous flow activated sludge test, Water Res. 34 (2000) 4101–4109.
[38] J. Wu, L. Ma, Y. Chen, Y. Cheng, Y. Liu, X. Zha, Catalytic ozonation of organic pollutants from bio-treated dyeing and finishing wastewater using recycled waste iron shavings as a catalyst: Removal and pathways, Water Res. 92 (2016) 140–148.
[39] H. Zhang, S. Song, Y. Jia, D. Wu, H. Lu, Stress-responses of activated sludge and anaerobic sulfate-reducing bacteria sludge under long-term ciprofloxacin exposure, Water Res. 164 (2019), 114964.
[40] J. Liu, Y. Yu, Y. Chang, B. Li, D. Bian, W. Yang, H. Huo, M. Huo, S. Zhu, Enhancing quinoline and phenol removal by adding Comamonas testosteroni bdq06 in treatment of an accidental dye wastewater, Int. Biodeterior. Biodegrad. 115 (2016) 74–82.
[41] N.R. Rane, V.V. Chandanshive, A.D. Watharkar, R.V. Khandare, T.S. Patil, P. K. Pawar, S.P. Govindwar, Phytoremediation of sulfonated Remazol Red dye and textile effluents by Alternanthera philoxeroides: An anatomical, enzymatic and pilot scale study, Water Res. 83 (2015) 271–281.
[42] G. Rangel-Sánchez, E. Castro-Mercado, E. García-Pineda, Avocado roots treated with salicylic acid produce phenol-2,4-bis (1,1-dimethylethyl), a compound with antifungal activity, J. Plant Physiol. 171 (2014) 189–198.
[43] J.M. Castillo, R. Nogales, E. Romero, Biodegradation of 3,4 dichloroaniline by fungal isolated from the preconditioning phase of winery wastes subjected to vermicomposting, J. Hazard. Mater. 267 (2014) 119–127.
[44] E. Padmini, L.R. Miranda, Nanocatalyst from sol–sol doping of TiO2 with Vanadium and Cerium and its application for 3,4 Dichloroaniline degradation using visible light, Chem. Eng. J. 232 (2013) 249–258.
[45] J. Liang, X.-A. Ning, J. Sun, J. Song, J. Lu, H. Cai, Y. Hong, Toxicity evaluation of textile dyeing effluent and its possible relationship with chemical oxygen demand, Ecotoxicol. Environ. Saf. 166 (2018) 56–62.
[46] A.R. Padmavathi, B. Abinaya, S.K. Pandian, Phenol, 2,4-bis(1,1-dimethylethyl) of marine bacterial origin inhibits quorum sensing mediated biofilm formation in the uropathogen Serratia marcescens, Biofouling 30 (2014) 1111–1122.
[47] A.R. Padmavathi, M. Periyasamy, S.K. Pandian, Assessment of 2,4-Di-tert-butyl-phenol induced modifications in extracellular polymeric substances of Serratia marcescens, Bioresour. Technol. 188 (2015) 185–189.
[48] A. Ventosa, R.R. de la Haba, C. Sánchez-Porro, R.T. Papke, Microbial diversity of hypersaline environments: a metagenomic approach, Curr. Opin. Microbiol. 25 (2015) 80–87.
[49] U. Sudarno, S. Bathe, J. Winter, C. Gallert, Nitrification in fixed-bed reactors treating saline wastewater, Appl. Microbiol. Biotechnol. 85 (2010) 2017–2030.
[50] I. Vyrides, D.C. Stuckey, Adaptation of anaerobic biomass to saline conditions: Role of compatible solutes and extracellular polysaccharides, Enzyme Microb. Technol. 44 (2009) 46–51.
[51] A. Uygur, F. Kargı, Salt inhibition on biological nutrient removal from saline wastewater in a sequencing batch reactor, Enzyme Microb. Technol. 34 (2004) 313–318.
[52] J. Xia, D.S. Wishart, Using MetaboAnalyst 3.0 for Comprehensive Metabolomics Data Analysis, Current Protocols in Bioinformatics, 55 (2016) 14.10.11-14.10.91.
[53] Y. Lv, J. Pan, T. Huo, Y. Zhao, S. Liu, Enhanced microbial metabolism in one stage partial nitritation-anammox system treating low strength wastewater by novel composite carrier, Water Res. 163 (2019), 114872.
[54] Y. Feng, Y. Zhao, B. Jiang, H. Zhao, Q. Wang, S. Liu, Discrepant gene functional potential and cross-feedings of anammox bacteria Ca. Jettenia caeni and Ca. Brocadia sinica in response to acetate, Water Res. 165 (2019), 114974.
[55] Y. Guo, Y. Zhao, T. Zhu, J. Li, Y. Feng, H. Zhao, S. Liu, A metabolomic view of how low nitrogen strength favors anammox biomass yield and nitrogen removal capability, Water Res. 143 (2018) 387–398.